A Scanning Electron Microscopy Study on the Morphologies of Isotactic Polypropylene Induced by Its Own Fibers

H. Li,† X. Zhang, X. Kuang, J. Wang, D. Wang, L. Li, and S. Yan*

State Key Laboratory of Polymer Physics and Chemistry, Institute of Chemistry, Chinese Academy of Sciences, Beijing 100080, P. R. China

Received December 17, 2003; Revised Manuscript Received February 26, 2004

ABSTRACT: The morphologies of iPP fiber/matrix homogeneity composites were studied on a lamellar level with the help of a field emission scanning electron microscope. It is found that the induced supermolecular structure of iPP depends strongly upon the fiber introduction temperature. At temperatures lower than 164 °C, no melting of the original iPP fiber takes place, and the solid iPP fiber can initiate only the growth of parallel aligned α-iPP lamellae normal to the fiber axis. At temperatures above 165 °C, the morphological change from the microfibrils to lamellae implies the occurrence of melting and recrystallization of the iPP fiber during sample preparation. At the same time, the increment of *β*-iPP content with the increase of fiber introduction temperature demonstrates unambiguously that the *β*-iPP crystallization is associated with the above-mentioned melting and recrystallization process. Combining the structural features of the recrystallized iPP fibers and the induced interfacial layers, it is suggested that the chain orientation status in the molten iPP fiber plays an important role in subsequent *β*-iPP crystallization.

Introduction

Isotactic polypropylene (iPP), as the first representative of the industrially manufactured stereoregular polymer, has been investigated extensively in the past few decades.[1−5] Concerning the polymorphous crystalline structures, α-iPP and *β*-iPP are its most classical crystalline modifications. However, its α-modification has attracted the most attention, for the iPP crystallizes predominantly in this form. The *β*-iPP, as a metastable phase, happens only under special crystallization conditions, such as temperature gradient, selective *β*-nucleating agents, and melt-shearing.[6−13] The crystal structure of *β*-iPP, formerly designated as a hexagonal system, was recently confirmed as a trigonal system.[14,15] Moreover, it has been demonstrated by several researchers that the presence of the *β*-form within the crystalline portion of the material is beneficial to its macroscopic toughness and ductility.[14,16−19] Therefore, more and more attention has been paid recently to this modification.

It was well documented that under many processing conditions, for example, injection-molding, extruding, and welding, shear stress is expected and leads to the formation of the familiar cylindritic structure with mixed polymorphic composition. Since an on-line observation of crystallization under the processing conditions meets technical difficulties, the fiber-pulling technique has been employed by many researchers to create and model the cylindritic crystallization under various thermal and mechanical conditions.[8−13] On the basis of systematic studies, it was concluded that the stretched macromolecules in melt under shear can produce α-iPP row nuclei. On the growth front of the in-situ formed α-row nuclei, growth of *β*-iPP modification may be initiated. This leads to the formation of cylindrites with mixed polymorphic composition. Varga and co-workers[13] reported that the polymorphous composition is not affected by the nucleation ability of the fibers but controlled by the temperature-dependent relative growth rate of the α- and *β*-iPP. The content of the *β*-modification is highest when the fiber-pulling and crystallization temperatures are closely matched within the temperature range of $T_{\alpha\beta}$ (α to *β* transition) ≈100 °C and $T_{\beta\alpha}$ (*β* to α transition) ≈140 °C.

In our previous studies,[20] through introducing the iPP fiber into its supercooled homogeneity matrix, the iPP fiber/matrix homogeneity composite was successfully prepared, and the resulting interfacial morphologies as a function of fiber introduction temperature were studied by optical microscopy. It was found that when introducing the fibers into its supercooled matrix at lower temperature, transcrystallization layers of purely α-iPP were produced. With increase of fiber introduction temperature, an increasing content of *β*-iPP surrounding the iPP fibers has been observed. At the fiber melting temperature, i.e., 173 °C, the induced interfacial layer was mainly composed of *β*-iPP. This is clearly somewhat different from the results obtained from the fiber-pulling experiments. To elucidate the formation mechanism of the *β*-iPP in our homogeneity composite system, fine interfacial structures on a lamellar level may be helpful. Therefore, the supermolecular structures of the iPP fiber/matrix homogeneity composites were studied in detail with the help of the field emission scanning electron microscope.

The purpose of this paper is to present some detailed morphological features of the iPP self-induced by its homogeneity fibers. Also, the growth mechanism of the *β*-iPP crystals is discussed on the basis of the obtained results.

Experimental Section

The iPP fiber/matrix homogeneity composites were produced by a procedure as shown in Figure 1. The iPP matrix thin film was first heated to 200 °C for 10 min to erase possible effects of thermal history of the sample on the subsequent crystal-

* To whom all correspondence should be addressed: e-mail skyan@iccas.ac.cn; Tel 0086-10-82618476; Fax 0086-10-62559373.
† Ph. D. candidates of the Chinese Academy of Sciences.

10.1021/ma035932c CCC: $27.50
Published on Web 03/16/2004

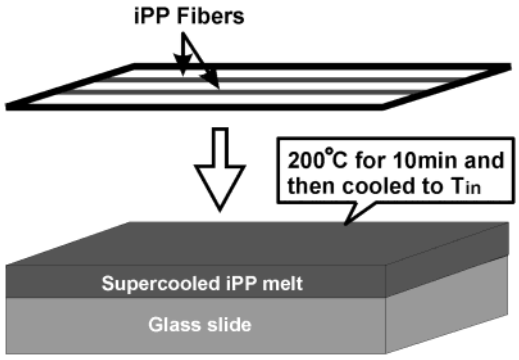

Figure 1. Sketch showing the sample preparation procedure.

lization and then moved to a preheated heat plate, where the iPP matrix was kept in the molten state or supercooled molten state at the moment of fiber introduction. As the iPP molten or supercooled molten thin layer reached an equilibrium at the desired temperature, homogeneity iPP fibers tightly fixed on a metal frame (as shown in Figure 1, upper part) were introduced into the iPP matrix. The fiber introduction temperatures used in this study were 158, 164, 168, and 173 °C. The obtained composites were then etched according to a procedure introduced by Basstt et al.[21] According to this method, mixed solvent was prepared by mixing two parts of sulfuric acid (98%) with one part of the phosphoric acid (85%). The etching reagent was then made by dissolving 1 wt % potassium permanganate into the above mixed solvent. Subsequently, the samples were etched for 3−4 h at room temperature, which is tested to be ideal for revealing the lamellar structure of iPP. After etching, the specimens were washed first with a mixture of sulfuric acid, water, and hydrogen peroxide with a ratio of 2:7:1 and then rinsed with distilled water and acetone several times. The samples were finally sputtered with a thin layer of gold after being dried in a vacuum oven.

For scanning electron microscopy (SEM) observation, a Hitachi S-4300 scanning electron microscope was used in this study.

The surface morphology of the original fibers was studied by using a Nanoscope III MultiMode atomic force microscope (AFM) (Digital Instruments) in a tapping mode. A typical value for the set-point amplitude ratio (r_{sp}) was 0.7−0.9. The amplitude of the free-oscillating cantilever was approximately 40 nm. TESP tips with a resonance frequency of approximately 300 kHz and a spring constant of about 30 N/m were used. The image presented in this work was subjected to a first-order plane-fitting and a first-order flattening procedures to compensate for the sample tilt.

Results and Discussion

It was well-known that in the composite systems of iPP matrix with some kinds of fibers in quiescent melts the fibers could serve as vast sites of heterogeneous nucleation and induce a quantity of lamellae to grow laterally. In our previous study,[20] it was found that when introducing the iPP fibers into the supercooled iPP melt at temperatures much lower than its melting point, the produced column layers in the vicinity of the fibers after isothermal crystallization were α-transcrystallization layers caused by heterogeneous nucleation. Since the fiber and matrix come from the same material, the transcrystallization layer of iPP matrix induced by its own fiber was quite uniform as observed by a polarized light microscope (PLM). However, owing to the limited resolution of PLM, many micromorphological features at the fiber/iPP matrix interface cannot be captured. Figure 2 shows a SEM micrograph of an iPP homogeneity fiber/matrix composite. The iPP fiber, which can be partially seen near the left side edge of the picture, was

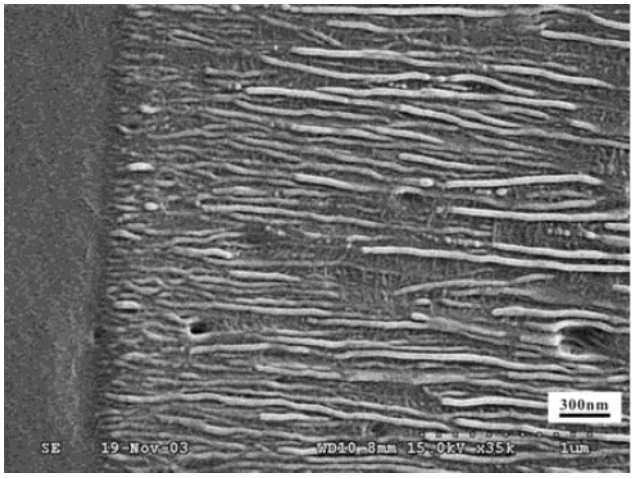

Figure 2. SEM micrograph of an iPP fiber/matrix composite prepared by introducing the iPP fiber into supercooled iPP matrix at 158 °C. The iPP fiber is located at the left side edge of the picture with fiber axis vertical. The iPP was isothermally crystallized at 135 °C for 1 h after the fiber introduction.

introduced into its supercooled homogeneity matrix at 158 °C. Its axial direction is vertical. The temperature for isothermal crystallization was set at 135 °C. From Figure 2, it can be observed that along the transverse section of the fiber there grow α-transcrystals. Between the fiber and the transcrystalline zone, a rather regular interface can be recognized. It is clearly illustrated that the transcrystalline zone is composed of edge-on lamellae with their growth direction normal to the fiber axis direction. Some of these lamellae are not continuous. This allows crystallization to occur in otherwise inaccessible regions. Between these parallel aligned lamellae, some branched lamellae in the longitudinal direction of the fiber can be observed. This reveals the characteristic crosshatched lamellar structure unique to α-iPP with the mother and daughter lamellae 80° apart from each other. The daughter lamellae grow via homoepitaxy on the lateral *ac* faces of the mother lamellae.[22,23] The daughter lamellae looks thinner than the mother ones, and further branching on the daughter lamellae has not been found. This may indicate that the daughter lamellae were most likely formed by the rejected materials during the cooling process of the sample. The lamellar structure of iPP in its homogeneity composite illustrated here is somewhat different from the row structures of α-iPP generated by shear flow. Bassett and co-workers have explored the microstructure of the row structure of α-iPP with lamellae resolution.[26] They reported that there is a proportion of lamellae, increasing with radial distance, which is more or less parallel rather than perpendicular to the core.

Optical microscope observations show that the transcrystals in Figure 2 were negative in birefringence. This is in accordance with the structural details observed by SEM. The optical character of iPP spherulites depends on two factors.[23] One of them is the relative proportion of the two populations of radial lamellae and tangential lamellae. The other one is the orientation of the radial lamellae relative to the path of light. In Figure 2, the edge-on radial lamellae confer a strong negative birefringence, while the edge-on tangential ones confer a strong positive birefringence to the transcrystals. Since the proportion of the former is much higher than that of the latter, a negative birefringence of the transcrystals in Figure 2 is expected.

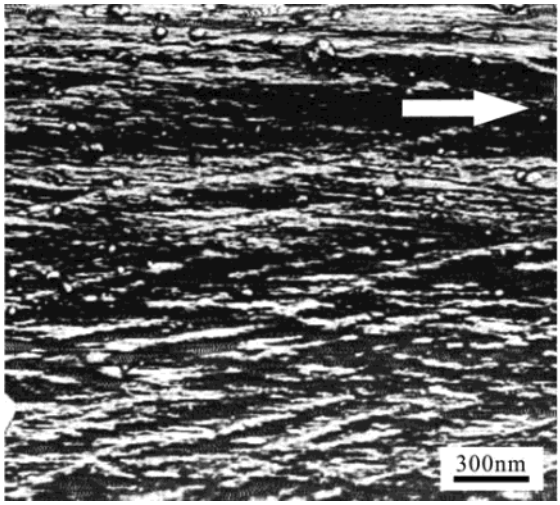

Figure 3. AFM phase image illustrating the surface structure of the used iPP fiber. The white arrow represents the axis direction of the fiber.

Moreover, it should be pointed out that the surface of the iPP fiber in Figure 2 is quite smooth, and no fine structures on a lamellar level can be detected. The same results were also obtained for the original iPP fiber either etched or unetched. Recently, many researchers have paid attention on the crystallographic and morphological features of the polypropylene fibers during melt-spinning process by atomic force microscopy (AFM).[24,25] The results illustrated a gradual transformation of the surface morphology from spherulites to fibrils during stretching. The transformation was realized by deformation of the original spherulites and then oriented lamellar stacks. The processing conditions influence the final morphology remarkably. To display the morphological feature of our used iPP fiber, AFM was employed to characterize the surface morphology of our homemade iPP fibers, which may be the key factor affecting the induced structure of the iPP matrix. As shown in Figure 3, the original fiber is mainly composed of microfibrils. These microfibrils are about tens of nanometers along the fiber axis direction and different in orientation from area to area of the same fiber.

Figure 4 shows the SEM micrographs of an iPP fiber/matrix homogeneity composite, which was prepared by introducing the iPP fiber into its supercooled homogeneity matrix at 164 °C and then isothermally crystallized at 135 °C for 1 h. In our previous optical microscopy study, it was found that both α- and *β*-iPP transcrystals could be produced around the iPP fibers at present condition with the fan-shaped *β*-iPP crystals dispersed randomly in the dominant α-iPP transcrystalline zone. This scene has also been observed by SEM with low magnification. As presented in Figure 4a, the iPP fiber about 25 um in diameter is located approximately in the central part of the picture. It exhibits still a fairly smooth surface. On its left side, one can see only α-iPP crystals growing normal to the fiber. On its right side, however, fan-shaped *β*-iPP crystals, which are separated from the fiber by a layer of saw-toothed α-iPP crystals, can be easily recognized. One may suggest that the α-iPP crystals were initially induced by the fiber. During the growth of these α-iPP crystals, nuclei in *β*-modification formed at the growth front of these α-iPP crystals and growth of *β*-iPP crystals started. Owing to the fast growth rate of *β*-iPP with respect to its α-counterpart,

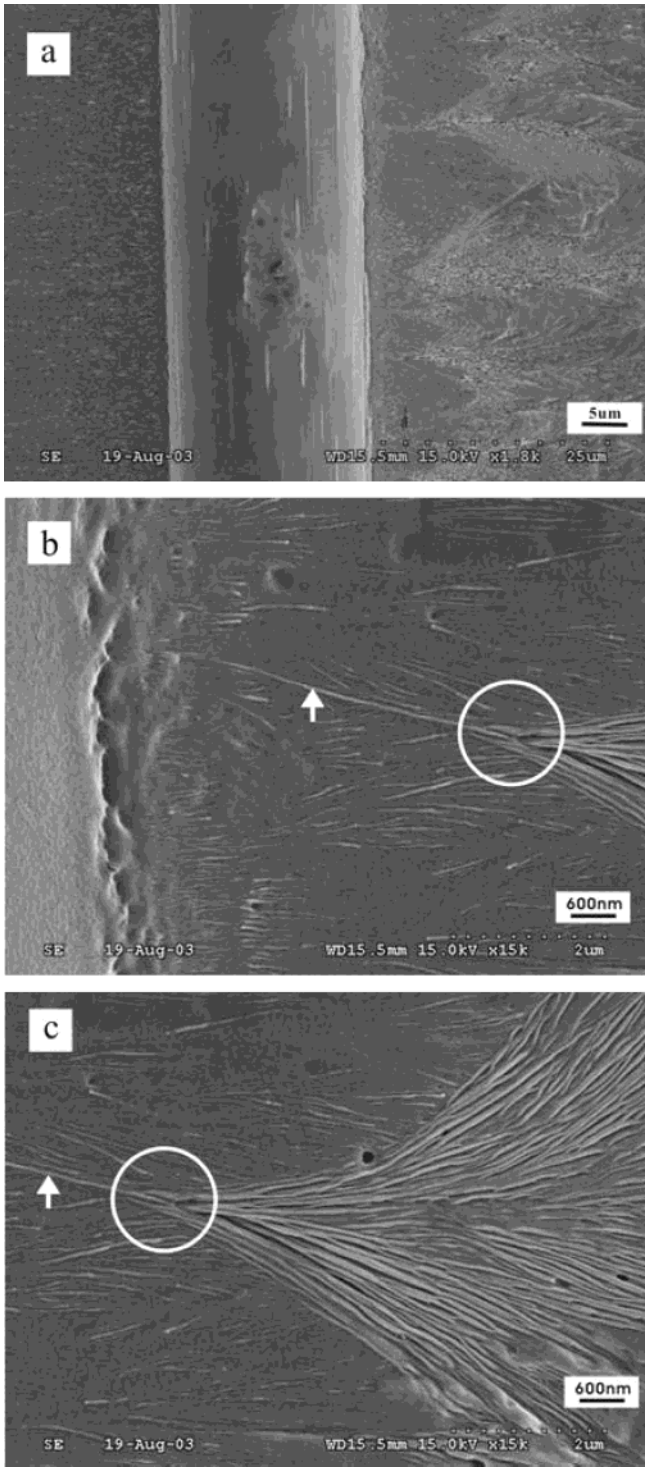

Figure 4. SEM micrographs of an iPP fiber/matrix homogeneity composite prepared by introducing the iPP fiber into its supercooled homogeneity matrix at 164 °C and then isothermally crystallized at 135 °C for 1 h. The white arrows indicate the initial single *β*-iPP lamella, while the circles outline the starting area of the fan-shaped *β*-iPP region.

the growth of the α-iPP has been hampered in a zigzag manner. The high-magnification SEM picture (Figure 4b) shows that the column structure in right part of Figure 4a is initially indeed comprised mainly of α-iPP lamellae grow normal to the fiber axis. However, among these α-iPP lamellae, there exists a single lamella, as indicated by an arrow, which starts from the interface and grows directly into the area where the fan-shaped *β*-iPP crystal started, as indicated by a circle. This single

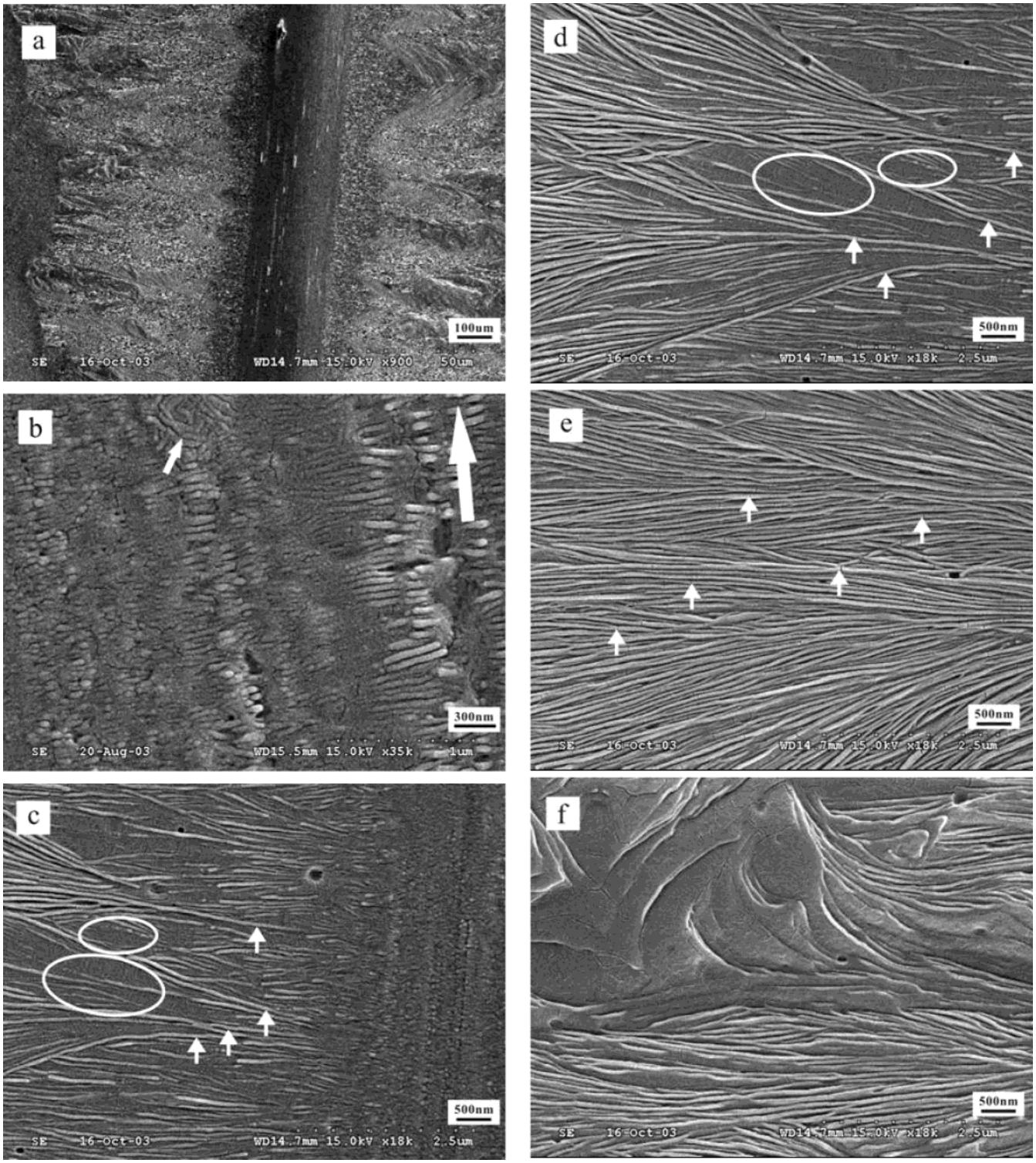

Figure 5. SEM micrographs of an iPP fiber/matrix composite prepared by introducing the iPP fiber into its supercooled homogeneity matrix at 168 °C and isothermally crystallized at 135 °C for 1 h. (a) An overall view at low magnification. (b) Surface lamellar structure of the iPP fiber with its axis being indicated by a big white arrow; a small white arrow labels the crosshatched lamellar structure which exists on the fiber surface. (c) Interfacial structure with the single β-iPP lamellae indicated by white arrows. (d) Growth of β-iPP at early stage. (e) Continuous growth of edge-on β-iPP lamellae with the nonperiodic cracks being indicated by white arrows. (f) Twisting of the β-iPP lamellae.

lamella should be assigned to its β-modification (more evidence can be found in Figure 5c,d, to be discussed later). The existence of this single lamella indicates that the β-iPP crystals nucleate and grow much earlier than that observed by the optical microscope. The growth process of the fan-shaped β-iPP crystals is well illustrated by Figure 4c. It is clear that several β-iPP lamellae are created after the single β-iPP lamella propagates for several micrometers. These initial β-iPP lamellae proliferate through branching and result in the formation of a fan-shaped β-iPP region. Some of the β-iPP lamellae are seen initially on edge and then converted flat-on through twisting about their width direction (see lower right corner of Figure 4c). This

observation is in good agreement with the result of Varga et al.[27] In Figure 4c, also the boundary between α- and β-iPP crystals has been clearly displayed. Because of the faster growth rate of β-iPP crystals, they splay out into the neighboring noncrystallized melt and stopped the growth of their α-counterparts. It is worth noting that no fine structure of iPP fiber can be identified here, too. Moreover, there are some grooves in the interfacial region between the fiber and the induced column structure. They may originate from sample preparation.

Figure 5 depicts the morphologies of an iPP fiber/matrix composite, which was prepared by introducing the iPP fiber into its supercooled matrix at 168 °C. There are several different morphological features of Figure 5 with respect to Figure 4. First of all, the iPP fiber looks different from the one shown in Figure 4. The difference can even be recognized at low magnification, comparing Figure 5a with Figure 4a. From the enlarged micrograph (Figure 5b), it is seen that the fiber consists of edge-on lamellae rather than microfibrils. Most of these lamellae are well arranged in the direction perpendicular to the fiber axis, while a small amount of them are more or less in the axial direction of the fiber, as indicated by a small white arrow, leading to the formation of α-iPP characteristic crosshatched structure. This unambiguously results from the melting and recrystallization of the fiber during sample preparation. Differential scanning calorimetry (DSC) measurements do indicate that the onset melting temperature of the iPP fibers is located at ca. 165 °C. The oriented recrystallization of iPP fiber can be explained as follow. The iPP fiber has been molten during fiber introduction. However, because of the high viscosity and short fiber introduction time (tens of seconds), the molten iPP fiber has not relaxed much. During the subsequent cooling process, the extended iPP chains serve as self-nuclei and induce the oriented recrystallization. Second, the content of β-iPP crystals is obviously increased (comparing Figure 5a with Figure 4a). Now the iPP fiber is completely surrounded by its β-crystals but fenced out by a narrow saw-toothed α-iPP layer. The detailed structural information about the α- and β-iPP crystals is better revealed by the parts c and d of Figure 5. It can be seen that large numbers of lamellae are initiated by the fiber and grow in the direction perpendicular to the fiber axis. Most of these lamellae are α-iPP crystals, which have been interrupted by the quickly formed β-iPP lamellae. A few of these lamellae, as indicated by the arrows in Figure 5c,d, grow from the α-iPP region continuously into the fan-shaped β-iPP region. This confirms that the growth of β-iPP crystals starts from a single lamella, which can propagate for several micrometers without any branching, and then splay out leading to the formation of fan-shaped structure. Third, at the beginning stage, the β-iPP lamellae are loosely packed with some α-iPP inclusion, as indicated by the ellipses in Figure 5c,d. This may be associated with the fast crystal growth but slower branching of the β-iPP lamellae. Indeed, comparing parts d and e of Figure 5, one can easily conclude that much less branches have been created at the beginning with respect to the later stage. It should be pointed out that at the initial stage the β-iPP lamellae bundles are separated from each other (Figure 5d), a situation similar to the nucleus of a spherulite. This may imply that these lamellae are created individually rather than branching. With further propagation of the β-iPP crystals, typical lamellae twisting occurs (see Figure 5f). Fourth, there exists no distinct boundary line between the fiber and iPP matrix anymore (compare Figure 5c with Figure 2). This confirms again the occurrence of at least a partial melting and recrystallization of iPP fiber, which may be the reason for the increment of β-iPP crystals. Another interesting thing should be addressed is the existence of the nonperiodic cracks, as indicated by white arrows in Figure 5e. The origin of them is unclear at the present moment.

It was documented that when the fiber introduction temperature is elevated to 173 °C, the induced column layer, or even some parts of the iPP fiber itself, of the obtained specimen is composed of fully β-iPP under an optical microscope. SEM observations of these samples are illustrated in Figure 6. From Figure 6a, it can be roughly recognized the existence of an induced crystallization zone in the middle of the picture, as outlined by two dashed white lines. Unlike the pictures presented above, the iPP fiber cannot be seen anymore. This results from the further melting of the iPP fiber. An overall scanning of this area with higher magnification shows that its central part is composed of purely β-iPP edge-on lamellae (Figure 6b), while its side regions are mainly composed of β-iPP flat-on crystals (Figure 6c), reflecting the twist of initial edge-on lamellae of Figure 6b. This is different from the optical microscopy observation, by which α-iPP crystals, more or less, can always be identified in the region where iPP fiber originally placed. The difference may stem from the different imaging principles. To confirm this, the sample used for Figure 6 was first quenched to room temperature from a heat treatment at 158 °C and then subjected the same etching process as previously performed. The SEM micrographs of the thus-prepared sample are presented in Figure 7. Now the outline of the original iPP fiber can be easily recognized (see Figure 7a). This confirms that the induced column layer is composed of purely β-iPP crystals. The high-magnification SEM image (Figure 7b) shows that the region of iPP fiber with brighter contrast consists of short poorly oriented α-iPP edge-on lamellae (compare Figure 7b with Figure 5b), while no fine structure is visible for the rest of the area. This demonstrates that the short α-iPP edge-on lamellae are formed previously rather than generated by selective melting and subsequent cooling process. In other words, these short α-iPP lamellae exist already in the sample of Figure 6 but covered by the β-iPP lamellae. After selective melting and etching the top thin layer away from the sample, these lamellae are clearly displayed. It is worth mentioning that the α-iPP fiber itself is partially molten out at 158 °C. This indicates the occurrence of transformation of iPP fiber from α-form into β-modification. Actually, the β-iPP lamellae covering the short α-iPP lamellae should also be converted from the original α-iPP fiber through melt recrystallization.

On the basis of the above results, the origin on the formation of β-iPP crystals can be discussed. First of all, it can be definitely concluded that the formation of β-iPP in our case is associated with the melting, or at least partial melting, and subsequent recrystallization of the iPP fiber. At a lower fiber introduction temperature, e.g. 158 °C, no melting event happens; only α-iPP crystals are initiated by the solid fiber via strong heterogeneous nucleation. As the fiber introduction

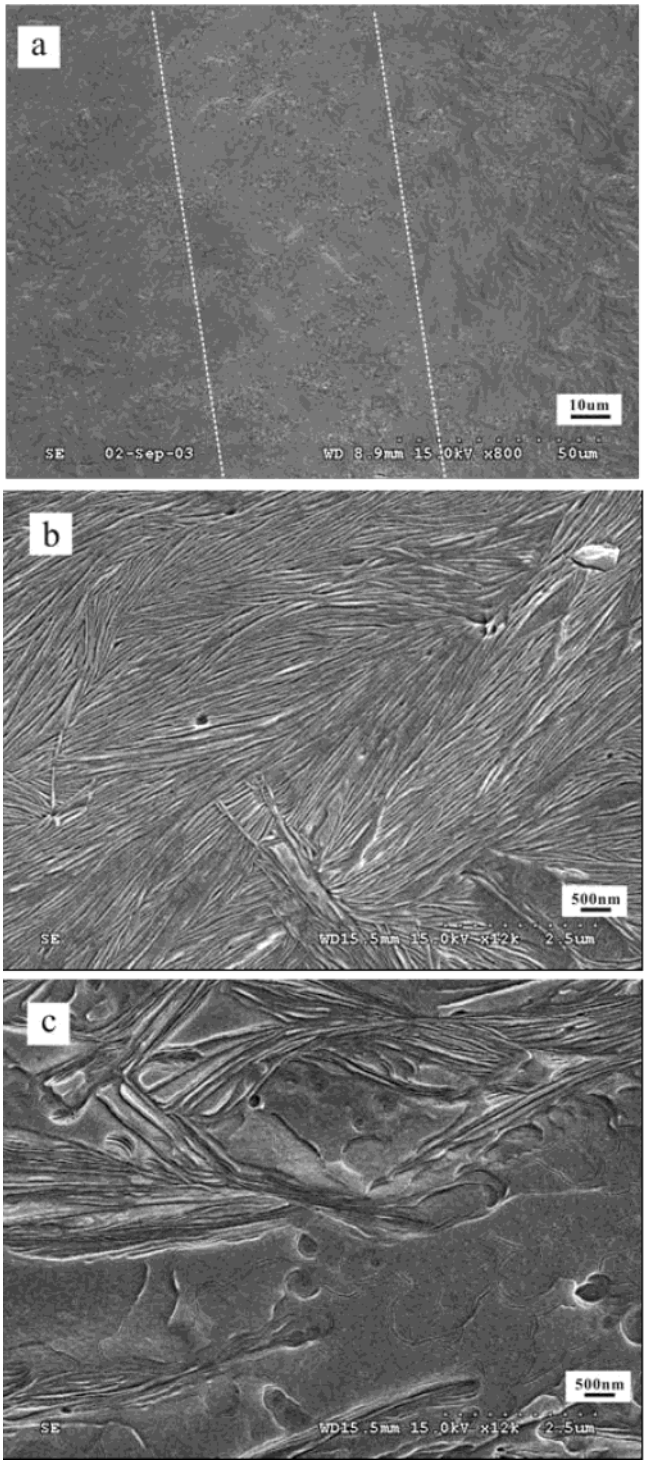

Figure 6. SEM micrographs of an iPP single polymer composite, of which the fiber introduction and isothermal crystallization temperatures were set at 173 and 135 °C, respectively. (a) An overall view at low magnification with the interfacial region outlined by two dashed white lines. (b) Lamellar structure of β-iPP at the top surface of the iPP fiber. (c) Morphology at the edge sides of the outlined area.

temperature elevated, e.g. 168 °C, the iPP fiber melts, or at least surface partial melts; meanwhile, the content of surrounding β-iPP crystals increases. When introducing the iPP fiber into its homogeneity matrix at 173 °C, around the melting temperature of the fiber, purely β-iPP crystals are induced, and even an α-to-β conversion has taken place. Moreover, the melting state of the fiber, or in other words, the chain orientation status in

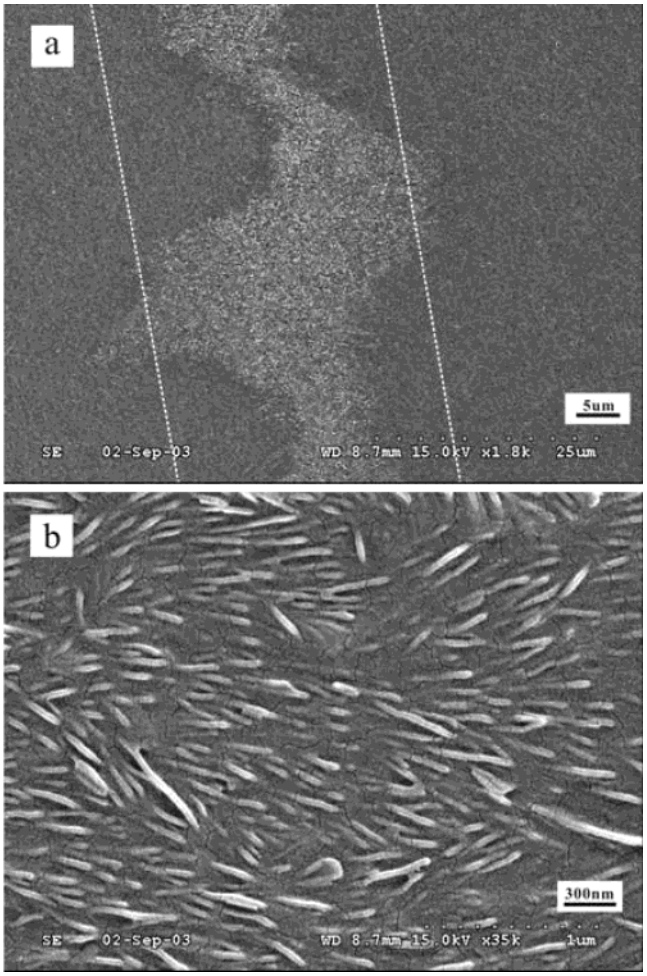

Figure 7. Micrographs of the sample used for Figure 5, which was quenched first to room temperature from a heat treatment at 158 °C and then subjected to the same etching process as previously performed. (a) An overall view at low magnification with the fiber location outlined by two dashed white lines. (b) Lamellar structure of α-iPP at top surface of the remaining iPP fiber.

the molten iPP fiber, may play a very important role in generating β-iPP crystals. At 168 °C, even though the melting and recrystallization of the iPP fiber take place, the iPP macromolecular chains do not relax much during that process. This leads to the formation of a complete β-iPP surrounding layer, which is fenced out from the fiber by a narrow saw-toothed α-iPP layer. At the fiber melting temperature, i.e., 173 °C, despite the short fiber introduction time, the molecular chains of iPP in the molten fiber are relaxed to some extent. As a result, pure β-iPP crystals are induced. It should be emphasized that, depending on the relaxation status, even some parts of the iPP fiber itself have been converted to the β-form through recrystallization. Another evidence for this argument is that mainly α-form iPP has been generated at temperatures higher than 173 °C, while only α-form iPP has been observed if the iPP fiber is completely relaxed, for instance at temperatures higher than 178 °C. According to the above discussion, the random dispersed fan-shaped β-iPP crystals in Figure 4 should be initiated by local chains which exhibit an orientation favorable β-crystallization.

Conclusions

From the morphological features revealed by SEM on a lamellar level, it can be concluded that the self-

induced β-iPP crystallization in its homogeneity composites is related to the melting and recrystallization of the iPP fiber. Solid iPP fiber can only initiate the growth of parallel aligned α-iPP lamellae perpendicular to its homogeneity fiber. If melting, or at least surface partial melting, and recrystallization of the iPP fiber take place, β-iPP crystals are the dominant interfacial morphology. The growth of β-iPP crystals can be initiated by a single edge-on lamella at the very beginning and then a bundle of separated edge-on β-iPP lamellae at the early stage. There exist α-iPP regions with characteristic crosshatched structure included in these sparsely packed β-iPP lamellae bundles. These β-iPP lamellae bundles spray out through branching and lead to the formation of a fan-shaped β-iPP crystalline region. With the propagation of edge-on β-iPP lamellae, twisting may occur about the width direction of the lamellae and result in the formation of multilayered β-iPP crystals. On the basis of the lamellar structure of the recrystallized iPP fiber, we speculated that it is the chain orientation status of the molten iPP fiber that plays a very important role in the subsequent β-iPP crystallization.

Acknowledgment. The financial support of the National Natural Science Foundation of China (No. 20304018 and 20374056) and the CAS hundred talents program is gratefully acknowledged.

References and Notes

(1) Brückner, S.; Meille, S. V.; Petraccone, V.; Pirozzi, B. *Prog. Polym. Sci.* **1991**, *16*, 361−404.
(2) Brückner, S.; Meille, S. V. *Nature (London)* **1989**, *340*, 455.
(3) Meille, S. V.; Brückner, S.; Porzio, W. *Macromolecules* **1990**, *23*, 4114.
(4) Padden Jr., F. J.; Keith, H. D. *J. Appl. Phys.* **1959**, *30*, 1479.
(5) Morrow, D. R.; Newman, B. A. *J. Appl. Phys.* **1968**, *39*, 4944.
(6) Lovinger, A. J.; Chua, J. O. Gryte, C. C. *J. Polym. Sci., Polym. Phys. Ed.* **1977**, *15*, 641.
(7) Shi, G. Y.; Zhang, X. D.; Qiu, Z. X. *Makromol. Chem.* **1992**, *193*, 583.
(8) Varga, J.; Karger-Kocsis, J. *Polym. Bull. (Berlin)* **1993**, *30*, 105.
(9) Varga, J.; Karger-Kocsis, J. *Polymer* **1995**, *36*, 4877.
(10) Varga, J.; Karger-Kocsis, J. *J. Mater. Sci., Lett.* **1994**, *13*, 1069.
(11) Varga, J. *J. Mater. Sci.* **1992**, *27*, 2557.
(12) Wu, C.; Chen, M.; Karger-Kocsis, J. *Polymer* **1999**, *40*, 4195.
(13) Varga, J.; Karger-Kocsis, J. *J. Polym. Sci., Polym. Phys.* **1996**, *34*, 657.
(14) Meille, S. V.; Ferro, D. R.; Brückner, S.; Lovinger, A. J.; Padden, F. J. *Macromolecules* **1994**, *27*, 2615.
(15) Lotz, B.; Kopp, S.; Dorset, D. *C. R. Acad. Sci. Paris* **1994**, *319*, 187.
(16) Varga, J. In *Polypropylene*: *Structure, Blends and Composites*; Karger-Kocsis, J., Ed.; Chapman & Hall: London, 1995, Vol. 1, Chapter 3.
(17) Karger-Kocsis, J. *Polym. Eng. Sci.* **1996**, *36*, 203.
(18) Karger-Kocsis, J.; Varga, J.; Ehrenstein, G. W. *J. Appl. Polym. Sci.* **1997**, *64*, 2057.
(19) Kotek, J.; Raab, M.; Baldrian, J.; Grellmann, W. *J. Appl. Polym. Sci.* **2002**, *85*, 1174.
(20) Li, H.; Jiang, S.; Wang, J.; Wang, D.; Yan, S. *Macromolecules* **2003**, *36*, 2802.
(21) Olley, R. H.; Bassett, D. C. *Polymer* **1982**, *23*, 1707.
(22) Padden Jr., F. J.; Keith, H. D. *J. Appl. Phys.* **1973**, *44*, 1217.
(23) Lotz, B. *J. Macromol. Sci.* **2002**, *B41*, 685.
(24) Hautojärvi, J.; Leijala, A. *J. Appl. Polym. Sci.* **1999**, *74*, 1242.
(25) De Rovère, A.; Shambaugh, R. L.; Órear, E. A. *J. Appl. Polym. Sci.* **2000**, *77*, 1921.
(26) White, H. M.; Bassett, D. C. *Polymer* **1997**, *38*, 5515.
(27) Varga, J. *J. Macromol. Sci.* **2002**, *B41*, 1121.

MA035932C